Selective Differentiation of Neural Progenitor Cells by High-Epitope Density Nanofibers

Gabriel A. Silva *et al.*

Science **303**, 1352 (2004);
DOI: 10.1126/science.1093783

Science (print ISSN 0036-8075; online ISSN 1095-9203) is published weekly, except the last week in December, by the American Association for the Advancement of Science, 1200 New York Avenue NW, Washington, DC 20005.

Selective Differentiation of Neural Progenitor Cells by High–Epitope Density Nanofibers

Gabriel A. Silva,[1]*† Catherine Czeisler,[2]* Krista L. Niece,[3] Elia Beniash,[3] Daniel A. Harrington,[3] John A. Kessler,[2] Samuel I. Stupp[1,3,4]‡

Neural progenitor cells were encapsulated in vitro within a three-dimensional network of nanofibers formed by self-assembly of peptide amphiphile molecules. The self-assembly is triggered by mixing cell suspensions in media with dilute aqueous solutions of the molecules, and cells survive the growth of the nanofibers around them. These nanofibers were designed to present to cells the neurite-promoting laminin epitope IKVAV at nearly van der Waals density. Relative to laminin or soluble peptide, the artificial nanofiber scaffold induced very rapid differentiation of cells into neurons, while discouraging the development of astrocytes. This rapid selective differentiation is linked to the amplification of bioactive epitope presentation to cells by the nanofibers.

Artificial three-dimensional (3D) scaffolds that store or attract cells, and then direct cell proliferation and differentiation, are of critical importance in regenerative medicine. Earlier work demonstrated that tissue regeneration using cell-seeded artificial scaffolds is possible, either by implanting the scaffolds in vivo or maintaining them in a bioreactor followed by transplantation (*1*–*9*). The scaffold materials used in most previous work have been biodegradable, nonbioactive polymers such as poly(L-lactic acid) and poly(glycolic acid) (*10*, *11*), as well as biopolymers such as collagen, fibrin, and alginate (*12*–*18*). The polymer scaffolds are typically prefabricated porous objects, fabrics, or films that are seeded with cells of the tissue to be regenerated. In the case of biopolymers, a common form of the scaffold is an amorphous gel in which cells can be encapsulated (*19*–*21*).

We report here on solid scaffolds that incorporate peptide sequences known to direct cell differentiation and to form by self-assembly from aqueous solutions of peptide amphiphiles. The scaffolds consist of nanofiber networks formed by the aggregation of the amphiphilic molecules, and this process is triggered by the addition of cell suspensions to the aqueous solutions. The nanofibers can be customized through the peptide sequence for a specific cell response, and the scaffolds formed by these systems could be delivered to living tissues by simply injecting a liquid (i.e., peptide amphiphile solutions that self-assemble in vivo). We show that an artificial scaffold can direct the differentiation of neural progenitor cells largely into neurons while suppressing astrocyte differentiation.

We used murine neural progenitor cells (NPCs) to study in vitro the use of a self-assembling artificial scaffold to direct cell differentiation (*22*). The choice of cell was motivated by the potential advantages of using NPCs to replace lost central nervous system cells after degenerative or traumatic insults (*23*–*26*). The molecular design of the scaffold incorporated the pentapeptide epitope isolucine-lysine-valine-alanine-valine (IKVAV), which is found in laminin and is known to promote neurite sprouting and to direct neurite growth (*27*–*35*). As a control for bioactivity we synthesized a similar molecule lacking the natural epitope, replacing it with the nonphysiological sequence glutamic acid–glutamine–serine (EQS) (*36*). As discussed below, these molecules form physically similar scaffolds by self-assembly, but cells encapsulated within the EQS gels did not sprout neurites or differentiate morphologically or histologically.

The chemical structure of the IKVAV-containing peptide amphiphile (IKVAV-PA) and a molecular graphics illustration of its self-assembly are shown in Fig. 1A, and a scanning electron micrograph of the scaffold it forms is shown in Fig. 1B. In addition to the neurite-sprouting epitope, the molecules contain a Glu residue that gives them a net negative charge at pH 7.4 so that cations in the cell culture medium can screen electrostatic repulsion among them and promote self-assembly when cell suspensions are added. The rest of the sequence consists of four Ala and three Gly residues (A_4G_3), followed by an alkyl tail of 16 carbons. The A_4G_3 and alkyl segments create an increasingly hydrophobic sequence away from the epitope. Thus, once electrostatic repulsions are screened by electrolytes, the molecules are driven to assemble by hydrogen bond formation and by the unfavorable contact among hydrophobic segments and water molecules.

The nanofibers that self-assemble in aqueous media place the bioactive epitopes on their surfaces at van der Waals packing distances (*37*, *38*). These nanofibers bundle to form 3D networks and produce a gel-like solid (Fig. 1, C to E). The nanofibers have high aspect ratio and high surface areas, 5 to 8 nm in diameter and with lengths of hundreds of nanometers to a few micrometers. Thus, the nanofibers that form around cells in 3D present the epitopes at an artificially high density relative to a natural extracellular matrix. Although we do not expect all of the epitopes to be available for receptor binding, we expect the molecularly designed scaffold to be a good vehicle for intense signal presentation to cells in 3D.

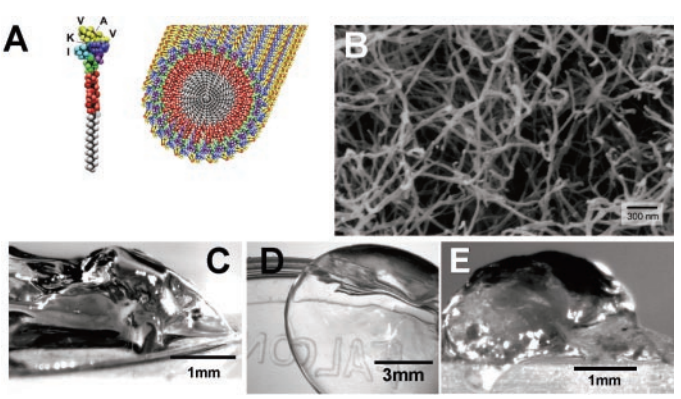

Fig. 1. (**A**) Molecular graphics illustration of an IKVAV-containing peptide amphiphile molecule and its self-assembly into nanofibers. (**B**) Scanning electron micrograph of an IKVAV nanofiber network formed by adding cell media (DMEM) to a peptide amphiphile aqueous solution. The sample in the image was obtained by network dehydration and critical-point drying of samples caged in a metal grid to prevent network collapse (samples were sputtered with gold-palladium films and imaged at 10 kV). (**C** and **D**) Micrographs of the gel formed by adding to IKVAV peptide amphiphile solutions (C) cell culture media and (D) cerebral spinal fluid. (**E**) Micrograph of an IKVAV nanofiber gel surgically extracted from an enucleated rat eye after intraocular injection of the peptide amphiphile solution.

[1]Institute for Bioengineering and Nanoscience in Advanced Medicine, [2]Department of Neurology, [3]Department of Materials Science and Engineering, [4]Department of Chemistry, Northwestern University, Chicago, IL 60611, USA.

*These authors contributed equally to this work.
†Present address: Jacobs Retina Center, University of California, San Diego, La Jolla, CA 92093–0946, USA. E-mail: gsilva@ucsd.edu
‡To whom correspondence should be addressed. E-mail: s-stupp@northwestern.edu

When 1 weight % (wt %) peptide amphiphile aqueous solution was mixed in a 1:1 volume ratio with suspensions of NPCs in media or physiological fluids, we obtained within seconds the transparent gel-like solid shown in Fig. 1, C and D (*39*). This solid contained encapsulated dissociated NPCs or clusters of the cells known as neurospheres (*22*). The cells survived the self-assembly process and remained viable during the time of observation (22 days) (Fig. 2, A to D) (*40*). There was no significant difference in viability between cells cultured on poly(D-lysine) (PDL, a standard substrate used to culture many cell types) relative to cells encapsulated in the nanofiber network (Fig. 2D). These results suggest that diffusion of nutrients, bioactive factors, and oxygen through these highly hydrated networks is sufficient for survival of large numbers of cells for extended periods of time. The artificial scaffolds formed by the self-assembling molecules contain 99.5 wt % water, and it is the high aspect ratio of the nanofibers that allows a mechanically supportive matrix to form at such low concentrations of the peptide amphiphiles. Thus, the artificial extracellular matrix not only provides mechanical support for cells but also serves as a medium through which diffusion of soluble factors and migration of cells can occur.

In the bioactive scaffolds, cell body areas and neurite lengths of NPCs that had differentiated into neurons as determined by immunocytochemistry (see below) showed statistically significant differences with respect to cells cultured on PDL- or laminin-coated substrates. Neurons within the nanofiber networks were noticeably larger than neurons in control cultures. The average cell body area of encapsulated progenitor cells in the networks was significantly greater after 1 and 7 days (Fig. 2E). Encapsulation in the nanofiber scaffold led to the formation of large neurites after only 1 day (about 57 ± 26 μm, mean ± SD), whereas cells cultured on PDL and laminin had not developed neurites at this early time. The neurons also had significantly longer processes in the scaffolds compared with cells cultured on the PDL substrates after 7 days ($P < 0.01$) (*41*). However, there was no statistical difference in neurite length between cells cultured on the PA scaffolds and cells cultured on laminin-covered substrates after 7 days. Transmission electron microscopy (TEM) of NPCs encapsulated in the bioactive scaffold for 7 days showed a healthy and normal ultrastructural morphology, including abundant processes visible in cross section throughout (Fig. 2F).

To assess the possibility of cell migration within the nanofiber scaffold, we tracked three encapsulated neurospheres for 14 days (Fig. 3, A and B). All three neurospheres spread out from their centers as constituent cells migrated outward (Fig. 3B). We quantified this effect by taking multiple measurements of the distance between the center of each neurosphere and the

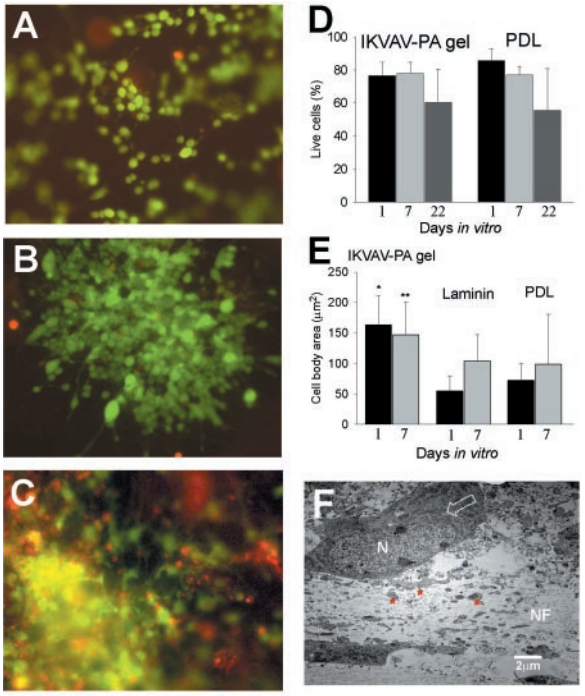

Fig. 2. Cell survival and morphology of NPCs encapsulated in IKVAV-PA gels or cultured on poly-(D-lysine) (PDL)-coated cover slips. Cell survival of encapsulated NPCs was determined by a fluorescent viability/cytotoxicity assay. Live cells fluoresce green due to the uptake and fluorescence of calcein in response to intracellular esterase activity; dead cells fluoresce red as a result of the entry of ethidium homodimer-1 through damaged cell membranes and subsequent binding to nucleic acids. Cell survival was determined at (**A**) 1 day, (**B**), 7 days, and (**C**) 22 days in vitro. (**D**) Quantification of cell survival expressed as a percentage of total cells. There was no difference in survival rates between experimental IKVAV-PA gels and PDL controls at any of the time points indicated. (**E**) Cell body areas of differentiated neurons in the IKVAV-PA gels were significantly larger than those of controls at both 1 and 7 days (*$P < 0.05$, **$P < 0.01$). (**F**) TEM of NPC encapsulated in an IKVAV-PA gel at 7 days. The cell has a normal ultrastructural morphology (N, nucleus; arrow, mitochondria). In addition, numerous processes can be seen in cross section (red asterisks) within the gel, surrounded by PA nanofibers (NF).

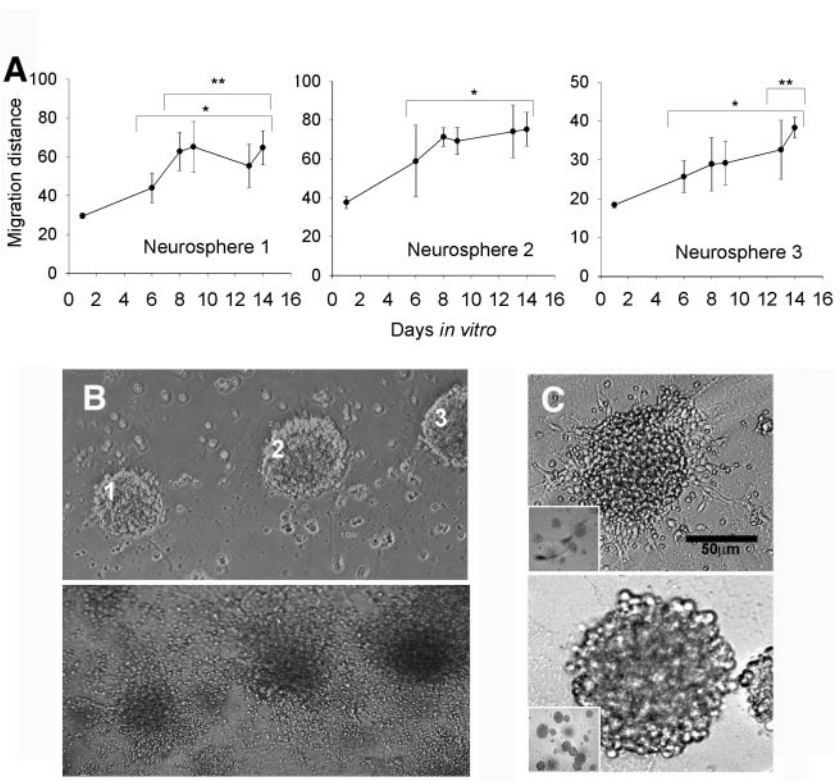

Fig. 3. Quantification of cell migration within a nanofiber network. (**A**) Quantification of the migration of NPCs from three representative neurospheres encapsulated in an IKVAV-PA gel. Migration distance is measured as distance (in μm) from the center of the neurosphere. (**B**) The three neurospheres for which the data in (A) were collected are shown at 1 day (top) and 14 days (bottom) in vitro. Similar results were observed for all IKVAV-PA–encapsulated neurospheres. (**C**) (Top) Brightfield image of an encapsulated NPC neurosphere in an IKVAV-PA gel less than 24 hours after plating. Neurite outgrowth is apparent, even at this early stage. (Bottom) By contrast, NPC neurospheres encapsulated in the control PA gel presenting the nonphysiological peptide sequence EQS did not show any neurite outgrowth. The insets show the (low-density) neurosphere cultures from which the two representative neurospheres in (C) were taken.

cell bodies at their outer perimeters (*42*), and individual cells could be seen to migrate away from the center of the cell mass. Migration of cells within the nanofiber matrix was statistically significant as a function of time ($P < 0.05$) (Fig. 3A). By contrast, NPCs encapsulated in denser, more rigid networks (98% as opposed to 99.5% water) did not survive. In the nonbioactive scaffolds containing nanofibers with the EQS sequence instead of the bioactive IKVAV sequence, cells failed to migrate away from the neurosphere even though they remained viable. A greater degree of neurite outgrowth was also observed in IKVAV-PA compared to the nonbioactive EQS-PA (Fig. 3C).

Immunocytochemistry was used to establish the in vitro differentiation of progenitor cells after 1 and 7 days in culture. We used β-tubulin III and glial fibrillary acidic protein (GFAP) markers for neurons and astrocytes [a subclass of central nervous system (CNS) glia], respectively (Fig. 4, A to E). As shown by immunocytochemistry, NPCs encapsulated in the network with nanofibers presenting IKVAV on their surface differentiated rapidly into neurons, with about 35% of total cells staining positive for β-tubulin after only 1 day. In contrast, there was very little GFAP+ astrocyte differentiation even after 7 days (<5%); inhibition of astrocyte proliferation is believed to be important in the prevention of the glial scar, a known barrier to axon elongation following CNS trauma (*43–45*).

The enhanced neuron numbers in the scaffold were detectable after only 1 day in culture and persisted after 7 days. In contrast, GFAP expression was significantly greater in cells cultured on PDL- and laminin-coated substrates relative to cells cultured on nanofiber networks (Fig. 4, F and G). Relative to PDL- or laminin-coated substrates studied previously (*46–49*), the IKVAV nanofiber scaffold promoted greater and faster differentiation of the progenitor cells into neurons. We established that the observed differentiation is specific to the IKVAV nanofiber networks by culturing the same cells within scaffolds formed by PA molecules containing the nonbioactive EQS sequence. In these scaffolds and in alginate [a gelatinous compound derived mostly from brown algae that has been well studied as a 3D matrix for various kinds of cells (*50–53*)], the encapsulated cells did not express quantifiable amounts of β-tubulin III or GFAP (*41*). As a further test of the 3D EQS control, we administered IKVAV soluble peptide into the EQS-PA–cell suspension mixture at concentrations of 100 μg/ml. Again, we did not observe selective neuron differentiation or cells sprouting neurites. Thus, the physical entrapment of the bioactive epitope in the self-assembled nanofibers, and not just its presence in the scaffold, is important in the observed cell differentiation.

To determine if the high density of bioactive epitope presented to cells is important in the observed rapid and selective differentiation, we carried out "titration" experiments using networks with varying amounts of IKVAV-PA and EQS-PA. We mixed four different increasing concentrations of the IKVAV-PA with EQS-PA to form the nanofiber scaffolds containing suspended NPCs as described before. The molar ratios used were 100:0, 90:10, 50:50, 40:60, and 10:90. We verified the presence of nanofibers in these mixed PA networks by TEM. The nanofibers of these networks contained either IKVAV-PA, or EQS-PA, or a mixture of both PA molecules. In either case, the key variable is the density of bioactive epitope in the cell environment. Immunocytochemistry data in these systems after 1 day (Fig. 4H) show that the available epitope density around the cells plays a key role in the observed neuron differentiation. We also investigated cell differentiation in nonbioactive EQS-PA scaffolds. In these scaffolds, titration with increasing amounts of soluble IKVAV peptide failed to induce the extent of neuron differentiation observed in IKVAV-PA nanofiber scaffolds (Fig. 4H), again showing that the presentation to cells of epitopes on the nanofibers is critical to the observed differentiation.

To understand the role played by 3D presentation of nanofibers to cells within the scaffold, we investigated NPC differentiation on a two-dimensional (2D) substrate coated with IKVAV-PA nanofibers. The PA molecules studied here self-assemble on surfaces upon drying (*37*, *38*), which we verified by TEM (*54*). Cells were plated for 1 day on these surfaces, and as shown by immunocytochemistry, the 2D surface was equally effective at inducing differentiation into neurons. Within experimental error, the percentage of cells that differentiated into neurons on the 2D substrates relative to the 3D scaffolds was the same (fig. S1). Substrates coated with IKVAV soluble peptide (*22*) or with laminin (Fig. 4) did not lead to the significant neuron differentiation observed on IKVAV-PA nanofibers in the same period. Indeed, the progenitor cells cultured on substrates coated with the IKVAV peptide expressed nearly nonquantifiable amounts of β-tubulin III and/or GFAP during the time of observation. These results suggest that nanofibers present to cells a high density of available epitopes, which promotes their differentiation either in 2D or 3D cultures. The findings point to density rather than dimension-

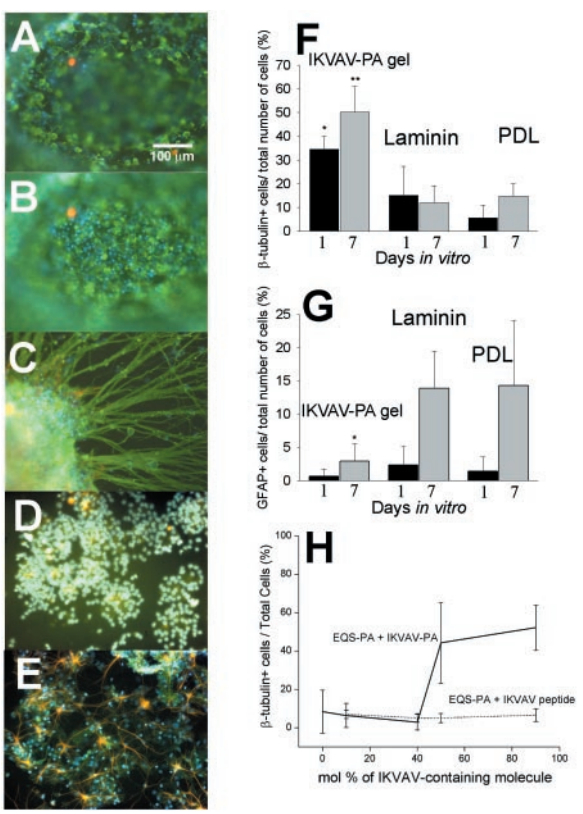

Fig. 4. NPCs cultured under different experimental conditions. (**A** and **B**) The same field of view in two different planes of focus showing immunocytochemistry of NPCs encapsulated in IKVAV-PA gels at 1 day. Differentiated neurons were labeled for β-tubulin (in green), and differentiated astrocytes (glial cells) were labeled for GFAP (in orange). All cells were Hoechst stained (in blue). (**C**) Immunocytochemistry of an NPC neurosphere encapsulated in an IKVAV-PA nanofiber network at 7 days. The large extent of neurite outgrowth was typical of the cells examined. (**D**) NPCs cultured on laminin-coated cover slips at 1 day. There is limited histological differentiation at this early stage. (**E**) NPCs cultured on laminin-coated cover slips at 7 days. The prevalence of astrocytes is apparent. Similar expression patterns were observed for NPCs cultured on poly-D-lysine–coated cover slips. (**F**) Percentage of total cells that differentiated into neurons (β-tubulin+). The IKVAV-PA gels had significantly more neurons compared to both laminin and poly-D-lysine (PDL) controls at both 1 and 7 days ($*P < 0.05$, $**P < 0.01$). (**G**) Percentage of total cells that differentiated into astrocytes (GFAP+). The IKVAV-PA gels had significantly fewer astrocytes compared to both laminin and PDL controls by 7 days ($*P < 0.05$). (**H**) Percentage of total cells that differentiated into neurons after 1 day in nanofiber networks containing different amounts of IKVAV-PA and EQS-PA (solid line) and in EQS-PA nanofiber networks to which different amounts of soluble IKVAV peptide were added (dashed line).

ality of epitope presentation as the key factor in the rapid and selective differentiation of cells into neurons. An average-sized nanofiber in the network contains an estimated 7.1×10^{14} IKVAV epitopes/cm^2. By contrast, closely packed laminin protein molecules in a two-dimensional lattice on a solid substrate have an estimated 7.5×10^{11} IKVAV epitopes/cm^2 (*22*). Thus, the IKVAV nanofibers of the network could amplify the epitope density relative to a laminin monolayer by roughly a factor of 10^3 (*22*).

The self-assembly of the scaffold studied here can also be triggered by injection of peptide amphiphile solutions into tissue. We injected 10 to 80 μl of 1 wt % peptide amphiphile solutions into freshly enucleated rat eye preparations and in vivo into rat spinal cords following a laminectomy to expose the cord (*22*). Thus, these peptide amphiphile solutions can indeed be transformed into a solid scaffold upon contact with tissues. This process localizes the network in tissue and prevents passive diffusion of the molecules away from the epicenter of an injection site. Furthermore, it is known that animals survive for prolonged periods after injections of the peptide amphiphile solutions into the spinal cord, a finding of relevance to the present study.

References and Notes

1. R. Langer, J. P. Vacanti, *Science* **260**, 920 (1993).
2. A. Lendlein, R. Langer, *Science* **296**, 1673 (2002).
3. Y. D. Teng *et al*., *Proc. Natl. Acad. Sci. U.S.A.* **99**, 3024 (2002).
4. L. Lu *et al*., *Biomaterials* **21**, 1837 (2000).
5. L. E. Niklason., *Science* **284**, 489 (1999).
6. S. Nehrer *et al*., *J. Biomed. Mater. Res.* **38**, 95 (1997).
7. A. Atala *et al*., *J. Urol.* **150**, 745 (1993).
8. H. L. Wald *et al*., *Biomaterials* **14**, 270 (1993).
9. I. V. Yannas, J. F. Burke, D. P. Orgill, E. M. Skrabut, *Science* **215**, 174 (1982).
10. D. J. Mooney *et al*., *Biomaterials* **17**, 1417 (1996).
11. A. G. Mikos, M. D. Lyman, L. E. Freed, R. Langer, *Biomaterials* **15**, 55 (1994).
12. E. Lavik, Y. D. Teng, E. Snyder, R. Langer, *Methods Mol. Biol*. **198**, 89 (2002).
13. W. C. Hsu, M. H. Spilker, I. V. Yannas, P. A. Rubin, *Invest. Ophthalmol. Vis. Sci.* **41**, 2404 (2000).
14. L. J. Chamberlain, I. V. Yannas, H. P. Hsu, G. R. Strichartz, M. Spector, *J. Neurosci. Res.* **60**, 666 (2000).
15. C. E. Butler, I. V. Yannas, C. C. Compton, C. A. Correia, D. P. Orgill, *Br. J. Plast. Surg.* **52**, 127 (1999).
16. D. P. Orgill *et al*., *Plast. Reconstr. Surg.* **102**, 423 (1998).
17. S. C. Chang *et al*., *J. Biomed. Mater. Res.* **55**, 503 (2001).
18. A. Atala *et al*., *J. Urol.* **150**, 745 (1993).
19. F. Lim, A. M. Sun, *Science* **210**, 908 (1980).
20. G. Hortelano, A. Al-Hendy, F. A. Ofosu, P. L. Chang, *Blood* **87**, 5095 (1996).
21. W. Xu, L. Liu, I. G. Charles, *FASEB J.* **16**, 213 (2002).
22. Materials and methods are available as supporting material on *Science* Online.
23. H. Okano, *J. Neurosci. Res.* **69**, 698 (2002).
24. A. Storch, J. Schwarz, *Curr. Opin. Invest. Drugs* **3**, 774 (2002).
25. M. F. Mehler, J. A. Kessler, *Arch. Neurol.* **56**, 780 (1999).
26. D. W. Pincus, R. R. Goodman, R. A. Fraser, M. Nedergaard, S. A. Goldman, *Neurosurgery* **42**, 858 (1998).
27. L. Kam, W. Shain, J. N. Turner, R. Bizios, *Biomaterials* **22**, 1049 (2001).
28. M. Matsuzawa, F. F. Weight, R. S. Potember, P. Liesi, *Int. J. Dev. Neurosci.* **14**, 283 (1996).
29. S. K. Powell *et al*., *J. Neurosci. Res.* **61**, 302 (2000).
30. T. Cornish, D. W. Branch, B. C. Wheeler, J. T. Campanelli, *Mol. Cell. Neurosci.* **20**, 140 (2002).
31. J. C. Chang, G. J. Brewer, B. C. Wheeler, *Biosens. Bioelectron.* **16**, 527 (2001).
32. B. C. Wheeler, J. M. Corey, G. J. Brewer, D. W. Branch, *J. Biomech. Eng.* **121**, 73 (1999).
33. L. Lauer, A. Vogt, C. K. Yeung, W. Knoll, A. Offenhausser, *Biomaterials* **23**, 3123 (2002).
34. P. Thiebaud, L. Lauer, W. Knoll, A. Offenhausser, *Biosens. Bioelectron.* **17**, 87 (2002).
35. C. K. Yeung, L. Lauer, A. Offenhausser, W. Knoll, *Neurosci. Lett.* **301**, 147 (2001).
36. The EQS peptide sequence has no known physiological signaling function but has a charge distribution that allows nanofiber self-assembly.
37. J. D. Hartgerink, E. Beniash, S. I. Stupp, *Science* **294**, 1684 (2001).
38. J. D. Hartgerink, E. Beniash, S. I. Stupp, *Proc. Natl. Acad. Sci. U.S.A.* **99**, 5133 (2002).
39. In vitro self-assembly was induced by addition of Dulbecco's minimum essential medium (DMEM), DMEM/F12, and modifications thereof, as well as by addition of cerebral spinal fluid.
40. Cell viability and toxicity was assessed using Molecular Probes Live/Dead assay (*22*).
41. G. A. Silva *et al*., data not shown.
42. G. Zhu, M. F. Mehler, P. C. Mabie, J. A. Kessler, *J. Neurosci. Res.* **59**, 312 (2000).
43. A. G. Rabchevsky, G. M. Smith, *Arch. Neurol.* **58**, 721 (2001).
44. Z. J. Chen, Y. Ughrin, J. M. Levine, *Mol. Cell. Neurosci.* **20**, 125 (2002).
45. S. Costa *et al*., *Glia* **37**, 105 (2002).
46. F. H. Gage, J. Ray, L. J. Fisher, *Annu. Rev. Neurosci.* **18**, 159 (1995).
47. M. Parmar, C. Skogh, A. Bjorklund, K. Campbell, *Mol. Cell. Neurosci.* **21**, 645 (2002).
48. S. Wu *et al*., *J. Neurosci. Res.* **72**, 343 (2003).
49. E. Alsberg, K. W. Anderson, A. Albeiruti, J. A. Rowley, D. J. Mooney, *Proc. Natl. Acad. Sci. U.S.A.* **99**, 12025 (2002).
50. L. Canaple, A. Rehor, D. Hunkeler, *J. Biomater. Sci. Polym. Ed.* **13**, 783 (2002).
51. S. C. Chang *et al*., *J. Biomed. Mater. Res.* **55**, 503 (2001).
52. J. J. Marler *et al*., *Plast. Reconstr. Surg.* **105**, 2049 (2000).
53. J. A. Rowley, D. J. Mooney, *J. Biomed. Mater. Res.* **60**, 217 (2002).

54. For 2D IKVAV-PA cell experiments, we first coated cover slips with PDL to ensure that the negatively charged IKVAV-PA nanofibers would adhere to the surface, and then placed 300 ml of 1 wt % aqueous solutions of the PA on surfaces and allowed them to dry overnight in a fume hood. We prepared the IKVAV peptide cover slips by spin-coating the peptide on the surface. The next day, all coated plates were washed three times with distilled water to remove any material not strongly adsorbed to the surface.

55. This material is based on work supported by the U.S. Department of Energy (grant DE-FG02-00ER45810/A001), NIH (grants NS20778, NS20013, and NS34758), and NSF (DMR-010-8342). Any opinions, findings, and conclusions or recommendations expressed in this work are those of the authors and do not necessarily reflect the views of these agencies.

Supporting Online Material

www.sciencemag.org/cgi/content/full/1093783/DC1
Materials and Methods
Fig. S1
References and Notes

18 November 2003; accepted 13 January 2004
Published online 22 January 2004;
10.1126/science.1093783
Include this information when citing this paper.

Carbon and Nitrogen Isotopic Anomalies in an Anhydrous Interplanetary Dust Particle

Christine Floss,[1]* Frank J. Stadermann,[1] John Bradley,[2] Zu Rong Dai,[2] Saša Bajt,[2] Giles Graham[2]

Because hydrogen and nitrogen isotopic anomalies in interplanetary dust particles have been associated with carbonaceous material, the lack of similar anomalies in carbon has been a major conundrum. We report here the presence of a ^{13}C depletion associated with a ^{15}N enrichment in an anhydrous interplanetary dust particle. Our observations suggest that the anomalies are carried by heteroatomic organic compounds. Theoretical models indicate that low-temperature formation of organic compounds in cold interstellar molecular clouds can produce carbon and nitrogen fractionations, but it remains to be seen whether the specific effects observed here can be reproduced.

Interstellar molecular clouds are the principal formation sites of organic matter in the Milky Way galaxy. A variety of simple molecules, such as CH_4, CH_3OH, and H_2CO, are produced in dense cold (10 to 30 K) clouds (*1*). At such low temperatures, where the difference in chemical binding energy exceeds thermal energy, mass fractionation produces molecules with isotopic ratios that can be anomalous relative to terrestrial values (*1–3*). Such anomalous ratios potentially provide a fingerprint for abiotic interstellar organic matter that was incorporated into the solar system and survives today in cosmically primitive materials such as interplanetary dust particles (IDPs).

IDPs collected in Earth's stratosphere are complex assemblages of primitive solar system material and carry various isotopic

[1]Laboratory for Space Sciences, Washington University, St. Louis, MO 63130, USA. [2]Institute for Geophysics and Planetary Physics, Lawrence Livermore National Laboratory, Livermore, CA 94550, USA.

*To whom correspondence should be addressed. E-mail: floss@wustl.edu